High Tc superconductors for plasmonics and metamaterials fabrication: A preliminary normal state optical characterisation of Nd123 and Gd1212

M. Gombos, S. Romano, I. Rendina, G. Carapella, R. Ciancio et al.

Citation: J. Appl. Phys. **114**, 083521 (2013); doi: 10.1063/1.4818942
View online: http://dx.doi.org/10.1063/1.4818942
View Table of Contents: http://jap.aip.org/resource/1/JAPIAU/v114/i8
Published by the AIP Publishing LLC.

JOURNAL OF APPLIED PHYSICS **114**, 083521 (2013)

High T_c superconductors for plasmonics and metamaterials fabrication: A preliminary normal state optical characterisation of Nd123 and Gd1212

M. Gombos,[1,2,a)] S. Romano,[1] I. Rendina,[1] G. Carapella,[2,3] R. Ciancio,[4] and V. Mocella[1]
[1]*CNR-IMM UOS Napoli, Napoli 80131, Italy*
[2]*Dip. di Fisica "E. R. Caianiello," Università di Salerno, Fisciano (SA) 84084, Italy*
[3]*CNR-SPIN UOS Salerno, Fisciano (SA) 84084, Italy*
[4]*CNR-IOM TASC Trieste, Basovizza (TS) 34149, Italy*

(Received 28 May 2013; accepted 5 August 2013; published online 29 August 2013)

The application of metamaterials and plasmonic structures in the visible and near infrared are strongly limited by the dissipative losses due to the low conductivity of the most used metals in this frequency range. High temperature superconductors are plasmonic materials at nonzero temperature that can provide a possible alternative approach to overcome this limit. Moreover, they can have zero or even negative dielectric constant, and a bipolar behavior. All these characteristics are attractive for plasmonic applications, and encourage further studies aimed at a more detailed knowledge of the parameters characterizing high temperature superconductors as possible optical materials. In this paper, Fourier Transform Infrared Spectroscopy analysis and ellipsometric measurements in the visible and infrared spectral regions on $NdBa_2Cu_3O_{7-\delta}$ (Nd123) and ruthenocuprate superconductor $GdSr_2RuCu_2O_{8-\delta}$ (Gd1212) are reported. As a matter of fact, Nd123 presents the highest transition temperature ($T_c = 96$ K) and the most interesting magnetic response properties among YBCO-like cuprate superconductors, whereas the coexistence in the same cell of superconductivity and magnetic order below T_c in Gd1212 can be an interesting feature for next metamaterial-like applications. The obtained results confirm the promising features of the considered materials. © *2013 AIP Publishing LLC*. [http://dx.doi.org/10.1063/1.4818942]

I. INTRODUCTION

Recently, and increasing interest has been devoted to metamaterials for the possibility of using them to develop new innovative optical devices.

Nanostructured materials present several unusual properties, such as negative or variable refraction index[1,2] that can be, for instance, exploited for cloaking applications[3–7] or slowing down electromagnetic waves[8] (giving a typical example of how, sometimes, scientific research may put into reality SCI-FI intuitions[9,10]). The main limitation preventing more widespread applications of these structures is the low conductivity of the generally used materials in the high (VIS and NIR) frequency range, which induce dissipative losses strongly affecting the device efficiency. A possible solution can be the substitution of conventional conductors, like gold, with high temperature superconductors (HTSC), which are expected to show better features in the frequency range of interest.

Superconductors are plasmonic materials[1,11–13] and present a number of interesting characteristics such as a negative dielectric constant correlated to the magnetic Meissner effect, and, depending on superconductor composition and doping, the possibility of exploiting two different charge carriers (*viz.*, holes and electrons).

Among HTSC compounds, the most diffused and studied are the YBCO-like hole-doped superconducting cuprate family RE123 ($REBa_2Cu_3O_{7-\delta}$, RE = Y, or Rare Earth),[14] whose Nd123 ($NdBa_2Cu_3O_{7-\delta}$) is the member characterized by the highest superconducting features.[15] In particular, Nd123 superconducting transition temperature (T_c) is 96 K. Moreover, it presents very interesting magnetic response features, such as a high (upper) critical magnetic field H_{c2}, and the appearance of a "fishtail effect" in locally non-superconducting samples[16] that is strictly correlated with the phenomenon, peculiar to Nd123, of cationic substitution.[17,18] The similarity of Ba^{2+} and Nd^{3+} ionic radii allows, indeed, a partial Nd-Ba substitution in Nd123 unitary cell leading to phases with an effective stoichiometry $Nd123(x) = Nd_{1+x}Ba_{2-x}Cu_3O_{7-\delta+x/2}$, that, in very low concentrations, can provide some additional pinning centres, so allowing higher critical currents at higher magnetic fields.[19] On the other side, Nd-Ba substitutions represent one of the most detrimentary features to Nd123 superconducting properties, because substituted phases present both critical temperature and critical magnetic fields lower than in the stoichiometric $x \approx 0$ one.[20] Substitutions also occur in Melt-Textured bulk samples by reaction of Nd123(0) with Nd422 ($Nd_4Ba_2Cu_2O_{10}$),[18,21] a phase generally added to Nd123 to increases its mechanical stability in the molten phase, and to provide pinning centres in the grown samples. Nd422 shows, indeed, a similar opposite tendency to form Ba-Nd substituted phases $Nd422(z) = Nd_{4-2z}Ba_{2+2z}Cu_{2-z}O_{10-2z}$. The occurring of this phenomenon may be prevented by using off-stoichiometric Nd422(0.2) ($Nd_{3.6}Ba_{2.4}Cu_{1.8}O_{9.6}$) that is almost at Ba solubility limit in Nd422 ($z_{min} \approx 0.2$)[21–23] and is then no more reactive with Nd123. A similar prevention effect is obtained by using Nd210 (Nd_2BaO_4) phase[21,22,24] that reacts with Nd123 forming Nd422(z_{min}) precipitates in the final samples.

a)marcello.gombos@cnr.it. Telephone +39 081 6132 285. Fax +39 081 6132598

The rutheno-cuprate compound Gd1212 ($GdSr_2RuCu_2O_{8-\delta}$) is structurally similar to Nd123 and is even more interesting as a possible metamaterial[25–27] because of the presence of Ru^{4+}–Ru^{5+} ions (in substitution of apical Re123 Cu^{2+}–Cu^{3+} ions) that order magnetically below 135 K.[28–30] This magnetic order, whose exact nature is still debated,[31–36] survives to the onset of superconductivity (at about 40 K depending on the fabrication procedures[37–39]), so that superconductivity and magnetic order coexist in the same cell below the superconducting transition temperature.

An accurate characterisation of these materials in the VIS and IR spectral regions is needed for a correct evaluation of their optical features and suitability as metamaterials.

In order to have more insight into these materials features, in this paper, we report about ellipsometric and Fourier Transform Infrared Spectroscopy (FTIR) measurements carried out in visible and infrared regime on Nd123- and Gd1212[40,41]- based Melt-Textured bulk samples, which present the best structural homogeneity and superconducting properties for these materials when in bulk form.[42–45]

II. SAMPLE FABRICATION

Three different kind of samples have been prepared for analysis: two different ones made from Nd123 (with the secondary Nd210 and Nd422(0.2) phases) and the third based on Gd1212 (and the secondary phase Gd1210 = $GdSr_2RuO_{5.5}$). Samples have all been grown, from precursor powders mixture sintered pellets, by means of Top-Seeded Melt-Textured Growth (TSG) technique, which allows to achieve large oriented domains with a high reproducibility.

Nd123 samples are centimeter sized single domains extracted from both single seeded TSG Nd123/Nd210 pellets and multiseeded TSG Nd123/Nd422(0.2) bars. Starting composition of powder mixture are Nd123 + 0.25 Nd210 for single seeded[24] and Nd123 + 0.25 Nd422(0.2) for multi seeded samples.[46,47] As already mentioned, the use of Nd422(0.2)[21–23] and Nd210[21,22,24] is due to the necessity of avoiding Nd-Ba cationic substitutions in Nd123. It has to be remarked that Nd123-Nd210 reaction produces also a small quantity of $NdBa_6Cu_3O_{10.5}$ (Nd163) phase,[48] rapidly decomposing into Nd123 plus oxides, and then with negligible effects on samples features. Other problems affecting Nd123 Melt-Textured samples, such as the formation of growth precipitate bands,[49] due to excessive adding of the secondary phase, and the problem of cracking and fragility of the largest size pellets,[50,51] have been taken into account in the choice of fabrication parameters, so that our samples do not present any remarkable problem under these aspects.

Gd1212 samples are multi-domain ones taken from multi domains TSG Gd1212/Gd1210 pellets.[40] Gd1210 is in relationship with Gd1212 in the same way of Nd442 with Nd123, being the solid phase produced in Gd1212 peritectic melting reaction[52,53]), so that its addition results necessary to achieve good superconducting properties.[39] Single domains in these pellets are, indeed, quite small (i.e., less than 0.5 mm), and of complex shape,[41] so that it was unpractical to extract them for our purpose. Gd1212 pellets starting composition is Gd1212 + 0.25 Gd1210.

The precursor powders: Nd123, Nd422(0.2), Nd210, Gd1210, and Gd1212 were separately produced by solid state reactions.[40,46,49] In particular, the two step procedure,[25] better discussed elsewhere,[39,53] was used for GdSrRuCuO compounds.

Precursor powders were then mixed by 2 h ball milling with the pure compounds in the chosen molar ratio, say Nd210:Nd123 = Nd422(0,2):Nd123 = Gd1210:Gd1212 = 1:4. The appropriate amounts of Nd123-based powder mixtures were uniaxially pressed into cylindrical pellets of about $Ø \approx 1$ cm diameter and $h \approx 8$ mm height, and into $1 \times 1 \times 5$ cm^3 bars. On their side, Gd1212-based powders mixture were uniaxially pressed into 2 g weight cylindrical pellets ($Ø \approx 1$ cm; $h \approx 4$ mm).

Single domain pellets were obtained by single seeded TSG technique, bars were obtained by multi-seeded TSG technique, both processes were performed in air.

Nd123 pellets were mounted on sintered CeO pedestals, with a thin protection layer of Y_2O_3 powder interposed.[49] Nd123 bars were mounted on pure Nd422(0,2) sintered pedestals. Gd1212 pellets were disposed over sapphire glass pedestals.

The seeds are squares of about $1 \times 1 \times 1$ mm^3 size cut from a commercial MgO single crystal slab. On pellets, they were simply placed at the centre of their top surface, whereas, on bars were positioned four seed, regularly spaced by about 1.6 cm in such a way to have their crystallographic axes parallel to the edges of the bar and to the upper surface normal.[46] Care was taken to maintain the same alignment for all seeds.

The processes are calibrated around the peritectic reaction temperature T_p. This is a partial melting reaction occurring for materials that, like cuprates and ruthenates, decompose into a solid and a liquid phase at high temperature. The peritectic reactions for Nd123 and Gd1212 in air are (in both formulas, L[X] indicates a liquid phase of X composition)

$$\mathrm{Nd123} = (1/4)\mathrm{Nd422(0)} + \mathrm{L}[(3/2)\mathrm{BaCuO_2} + \mathrm{CuO}] \quad (1)$$

occurring at $T_p = 1095\,^{\circ}C$ for Nd123,[42] and

$$\mathrm{Gd1212} = \mathrm{Gd1210} + \mathrm{L[CuOx]} \quad (2)$$

occurring at $T_p = 1117\,^{\circ}C$ for Gd1212.[52,54]

Samples were completely molten in a muffle furnace for 5 h at the melting temperature $T_m > T_p$. To obtain presintered high-density pellets, and preventing cracks formation before melting, T_m was reached by a two step ramp: 300 °C/h up to 800 °C and then further up at 60 °C/h.

Furnace was cooled to the first undercooling temperature T_1, where it dwelt for 2 h, and then, by a growth cooling rate C_{12} to the second undercooling temperature T_2, where stayed for 1 h to ensure a complete growth.

For Nd123-based samples, $T_m = 1135\,^{\circ}C$, $T_1 = 1075\,^{\circ}C$, and $T_2 = 1060\,^{\circ}C$, while $C_{12} = 0.6\,^{\circ}C/h$ for the pellets and $C_{12} = 0.5\,^{\circ}C/h$ for the bars. On their side, Gd1212-based samples schedule thermal parameters are $T_m = 1190\,^{\circ}C$, $T_1 = 1130\,^{\circ}C$, $T_2 = 1115\,^{\circ}C$, and $C_{12} = 0.5\,^{\circ}C/h$.

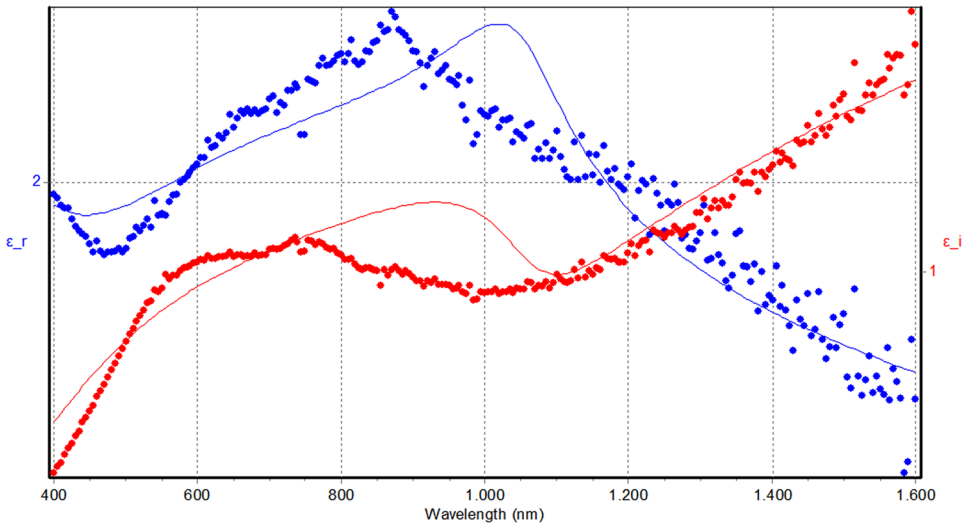

FIG. 1. ε_r (blue) and ε_i (red) values measured on a single domain fragment of a Nd123-based TS-MTG bar: values were reconstructed from the ψ, Δ raw data by the usual DeltaPsi2 program. Measurements were performed in an incidence angle of 70° with the detectors disposed specularly to the source. Data show the hybrid nature of the material, presenting a conducting Drude component and an insulating Lorentz one. Solid lines are the numerical curves obtained by the best fit procedure.

Finally, furnace was cooled to room temperature. The whole process was performed in air.

To ensure that both materials are in the structurally correct phase, Nd123 samples were annealed at 420 °C for 12 h in pure oxygen flux.

To avoid light scattering resulting in an insufficient reflectivity, the upper surfaces of all samples have been polished by cloths down to a 1 μm grain.

III. OPTICAL CHARACTERISATION

Normal state properties of bulk Melt-Textured Nd123 and Gd1212 cuprate superconductors have been analysed by visible and infrared spectroscopies. The interest in analysing HTSC in the normal state is related to the presence of a superconducting pseudogap up to room temperature and beyond.[55,56] Moreover, these analyses allow a more precise calibration useful for further investigation at lower temperature. The optical properties of the samples have been investigated at room temperature by using a Jobin Yvon—Horiba UVISEL VUV to NIR Spectroscopic Ellipsometer operating in the visible and near infrared range between 400 nm and 1600 nm. Ellipsometric measurements have been performed on a domain extracted by a Nd123-Nd422 bar and confronted with the ones obtained by analysing Nd123-Nd210 and Gd1212-Gd1210 pellets. In the investigated VIS and NIR range, polished pellets appear shiny black because of high light absorption. Great care was then devoted in positioning correctly the sample, even because slight deformations occurred during the thermal treatment. In fact, the upper surface of the bar fragment can be not perfectly horizontal, with deviations from the vertical up to 4°[47] (to be compensated). Ellipsometric spectra are reported in Fig. 1. They show a quite interesting characteristic given by an almost simple profile that, anyway, is not immediately attributable to a pure Drude (conducting) or Lorentz (insulating) behaviour. The real part of the permittivity, ε_r, starts decreasing at 400 nm until reaching a minimum of 1.8 at about 480 nm. Then, it increases almost monotonically up to 2.3 at about 850 nm, where it reaches its local maximum, before decreasing again in the 850–1600 nm range. The imaginary part ε_i increases between 400 and 550 nm, then stays around 1 up to about 1100 nm, where it starts to increase again up to about 1.9 at 1600 nm.

Collected data have been analysed by the DeltaPsi2 software and fitted to obtain a model of the room temperature optical behaviour. An hybrid model was used, composed by a Drude component, accounting for the conducting behavior (and, with the appropriate modifications, for the superconducting one below T_c), and a Lorentz oscillator component accounting for the insulator behaviour. This model slightly modifies the one used in classical works on YBCO.[57,58] A two fluids Drude model,[59] accounting for the superconducting and the normal state components, or even a more complex one,[60] is expected to better describe the optical behavior in the superconducting regime.

The following formula was used to model our samples (the coefficients are due to the normalisation applied in the fitting program):

$$\varepsilon = 0.5\,\varepsilon_\infty + 0.25\,\mathrm{D}(\omega) + 0.25\,\mathrm{L}(\omega), \tag{3}$$

where ε_∞ is the constant value that permittivity achieves at higher frequencies.

TABLE I. χ^2 minimization on ε_r, ε_i. Fitting has been made by an hybrid model, combining an insulating Lorentz oscillator component with a conducting Drude one.

Parameters	Value	Notes
χ^2	0.011517	
epsilon %	50%	Fixed[a]
epsilon2 ε_∞	1.1386610	
Drude %	25%	Fixed[a]
Drude model ω_p	521.2909000 nm	
Drude model Γ_d	1286.6810000 nm	
Lorentz %	25%	Fixed[a]
Lorentz oscillators N_{osc}	0.6276293 $eV^{-2}nm^{-1}$	
Lorentz oscillators ω_0	1.8977460 nm	
Lorentz oscillators γ	0.2790371 nm	
Lorentz oscillators ν	4.3250000	
Lorentz oscillators Φ	−0.1042017	

[a]Post fit re-fitting of these values 1eft them unchanged.

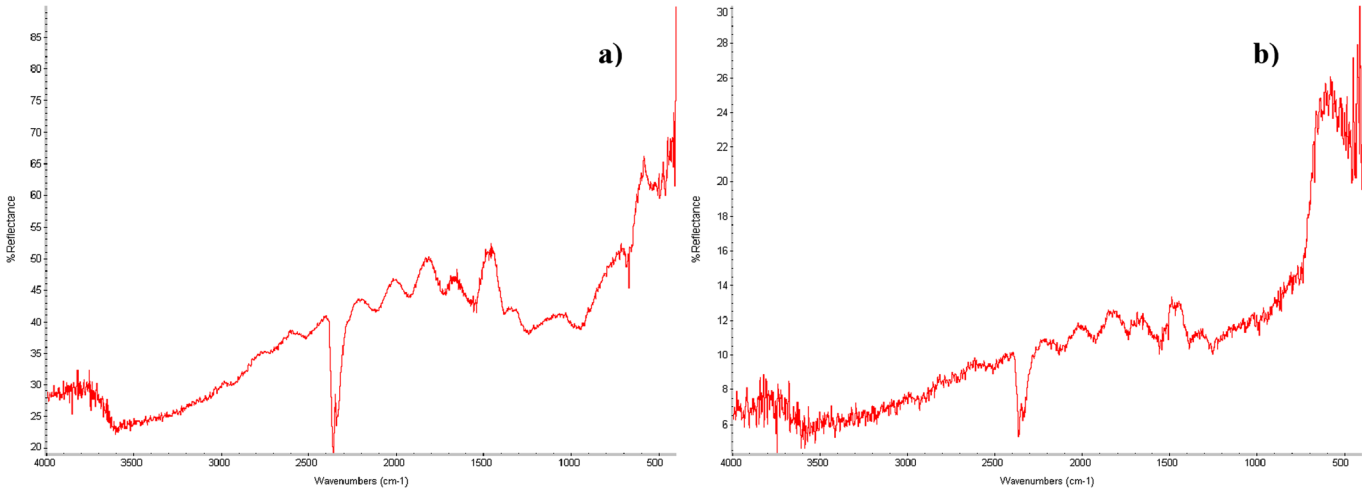

FIG. 2. (a) FTIR analysis performed on a single domain Nd123 pellet in the MIR range (4000–400 cm^{-1}); (b) FTIR analysis performed on a multidomain Gd1212 pellet in the MIR range (4000–400 cm^{-1}). In both images, the peak around 2400 cm^{-1} is a background one. Slight undulations in the 2300–1000 cm^{-1} range form a band structure correlated to charge carrier and spin stripes in superconductors.[61]

$$D(\omega) = \frac{\omega_p^2}{\omega^2 + i\omega\Gamma_d} \tag{4}$$

and

$$L(\omega) = \frac{H(\omega)}{1 - \nu H(\omega)} \tag{5.1}$$

are the Drude model formula for the free charge carriers and the Lorentz oscillators formula, respectively, with

$$H(\omega) = \frac{N_{osc} \cdot 1.37886 eV^2 nm^3}{\omega_0^2 - \omega^2 - i\gamma\omega} e^{i\Phi}. \tag{5.2}$$

In the Drude formula, ω_p is the plasma frequency and Γ_d is the damping coefficient of the free electron gas. In the Lorentz formula, N_{osc} is proportional to the squared oscillator strength,[57] ν is the oscillators number, ω_0 is the oscillator frequency, γ is the oscillator damping coefficient, and Φ is a phase term.

The fit analysis has been performed in several subsequent steps, minimizing each component both separately and jointly with the others, each time putting the results of the previous run as the starting point for the next one, until a good correspondence of fitted curves with experimental data appeared.

For the first run, we tried several hypothetical values for the plasma frequency ω_p ranging around the maximum between 700 and 1000 nm: in all cases, at the end of the whole process, the results tended to the values shown in Table I. The same occurred for the hypothetical values of the Lorentz oscillators parameters. A final control on the fitting weights has been performed after the last step, but the results confirmed the validity of the initial choice.

The fitting results are shown in Table I. They show a Drude plasma frequency not so far from the expected one. Moreover, a high Lorentz oscillators frequency is also obtained.

FTIR analysis has been performed on our samples, by means of a Thermo Nicolet Nexus FTIR. Spectra were collected

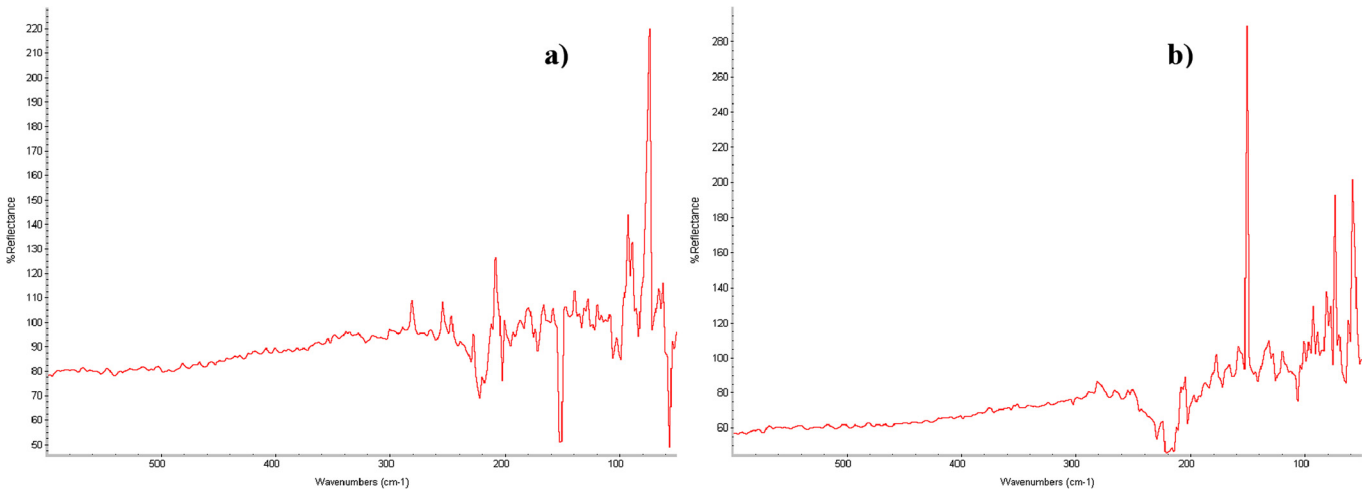

FIG. 3. (a) FTIR analysis performed on a single domain Nd123 pellet in the FIR range (600–50 cm^{-1}). (b) FTIR analysis performed on a multidomain Gd1212 pellet in the FIR range (600–50 cm^{-1}). Structures are observed only in the longest wavelength range. The large plateau for wavenumbers higher than about 300–250 cm^{-1} (λ smaller than about 33 000–40 000 nm $\approx$ eV) is the signal of the presence of a superconducting pseudogap at room temperature.

in the far-infrared (FIR) and in the mid-infrared (MIR) ranges that mean, respectively, $600\,cm^{-1} > k > 50\,cm^{-1}$ corresponding to about $16\,000\,nm < \lambda < 200\,000\,nm$ (Figs. 2(a) and 2(b)) and $4000\,cm^{-1} > k > 400\,cm^{-1}$ corresponding to about $2500\,nm < \lambda < 25\,000\,nm$ (Figs. 3(a) and 3(b)).

Both Nd123 and Gd1212 spectra show an articulated peaks structure only in the FIR range region with k smaller than about 250–300 cm−1 or equivalently λ bigger than about 33 000–40 000 nm, whereas in the MIR range, and in the nearest FIR range (k bigger than about 300–250 cm^{-1} or λ smaller than about 33 000–40 000 nm) does not appear any remarkable structure, coherently with which observed by other authors.[56] Only the slight undulation visible in the 2300–1000 cm^{-1} range (4300–10 000 nm) may resemble the band structure observed by other authors and correlated to charge carrier and spin stripes in superconductors.[61]

IV. CONCLUSIONS

The search of materials not subject to the high frequency limitations of conventional conductors is fundamental in the development of metamaterials to be exploited in the design of new devices. For this purpose, we have focused the attention on the characterization of two of the most promising High Temperature Superconductors (HTSC): the cuprate Nd123 ($NdBa_2Cu_3O_{7-\delta}$) and the, almost isostructural, ruthenocuprate Gd1212 ($GdSr_2RuCu_2O_{8-\delta}$). Gd1212, in particular, is especially promising, due to the observed coexistence of superconductivity and magnetic ordering in its unitary cell. This feature may lead, indeed, to unconventional effects, useful for innovative plasmonic structures and devices.

We have chosen to start our investigation from the normal state behavior of crystal oriented, bulk melt textured samples, in order to gradually approximate the complex behaviour of HTSC in the superconducting state below T_c. By this approach, we have begun to observe the effects due to the presence of a pseudogap also at room temperature, a competing effect to superconductivity whose observation in ruthenocuprate Gd1212 is of high interest.

We performed FTIR and ellipsometric measurements on melt-textured samples of the chosen superconducting materials, obtained by means of Top-Seeded Melt-Texturing technique (TSG). In particular, for Nd123, we analyzed two different kind of samples: single domains taken from Nd123-Nd422 Multi-Seeded TSG bars and Nd123-Nd210 single-seeded TSG pellets. Measurements on Gd1212 TSG pellets have been made, instead, on a multi domain sample, due to the difficulty of extracting the single domains.

The analysis of the results of the ellipsometric measurement of the permittivity spectra, in the visible and NIR optical ranges, stress the need to take into account both the conducting and the insulating behavior of the materials. This has been done using a hybrid model with both Drude and Lorentz oscillators components.

FTIR measurements show a low reflectivity in the MIR and in the nearest FIR ranges, due to the presence of a superconducting pseudogap. The slight undulation visible in the spectra in the MIR range may be probably correlated with charge carrier stripes.

It is important to say that, due to the high similarity of their crystal structure and parameters, no significant differences appeared among Gd1212 and both kinds of Nd123 samples in these conditions. We suppose that some divergences could appear analyzing the magnetic ordered and the superconducting regimes.

These results confirm the very promising aspects of HTSCs for metamaterials fabrication; further analyses of our samples in lower temperature regimes, and the extension of this study to powders and films, are in progress.

[1]A. Tsiatmas, A. R. Buckingham, V. A. Fedotov, S. Wang, Y. Chen, P. A. J. de Groot, and N. I. Zheludev, "Superconducting plasmonics and extraordinary transmission," Appl. Phys. Lett. **97**, 111106 (2010).

[2]W. T. Lu, S. Savo, B. Didier, F. Casse, and S. Sridhar, "Slow microwave waveguide made of negative permeability metamaterials," Microwave Opt. Technol. Lett. **51**, 2705–2709 (2009).

[3]D. Shin, Y. Urzhumov, Y. Jung, G. Kang, S. Baek, M. Choi, H. Park, K. Kim, and D. R. Smith, "Broadband electromagnetic cloaking with smart metamaterials," Nat. Commun. **3**, 1213 (2012).

[4]N. Landy and D. R. Smith, "A full-parameter unidirectional metamaterial cloak for microwaves," Nature Mater. **12**, 25–28 (2013).

[5]G. DiCaprio, P. Dardano, G. Coppola, S. Cabrini, and V. Mocella, "Digital holographic microscopy characterization of superdirective beam by metamaterial," Opt. Lett. **37**, 1142–1144 (2012).

[6]P. Dardano, M. Gagliardi, I. Rendina, S. Cabrini, and V. Mocella, "Ellipsometric determination of permittivity in a negative index photonic crystal metamaterial," Light Sci. Appl. **1**, e42 (2012).

[7]V. Mocella, P. Dardano, I. Rendina, and S. Cabrini, "An extraordinary directive radiation based on optical antimatter at near infrared," Opt. Express **18**, 25068–25074 (2010).

[8]S. Savo, W. T. Lu, B. Didier, F. Casse, and S. Sridhar, "Observation of slow-light in a metamaterials waveguide at microwave frequencies," Appl. Phys. Lett. **98**, 171907 (2011).

[9]B. Shaw, "Light of other days," Analog **77** (1966)

[10]B. Shaw, *Other Days, Other Eyes* (Ace Books, New York, 1972).

[11]A. H. Majedi, "Theoretical investigations on THz and optical superconductive surface plasmon interface," IEEE Trans. Appl. Supercond. **19**, 907–910 (2009).

[12]P. Sabatino, G. Carapella, and M. Gombos, "Preferentially directed flux motion in a very thin superconducting strip with nanostructured profile," J. Appl. Phys. **112**, 083909 (2012).

[13]P. Tassin, T. Koschny, M. Kafesaki, and C. M. Soukoulis, "A comparison of graphene, superconductors, and metals as conductors for metamaterials and plasmonics," Nat. Photonics **6**, 259–264 (2012).

[14]J. L. MacManus-Driscoll, "Material chemistry and thermodynamics of $REBa_2Cu_3O_{7-x}$," Adv. Mater. **9**, 457–473 (1997).

[15]S. I. Yoo and R. W. McCallum, "Phase diagram in the Nd-Ba-Cu-O system," Physica C **210**, 147 (1993).

[16]S. Li, E. A. Hayri, K. V. Ramanujacharry, and M. Greenblatt, "Orthorhombic-to-Tetragonal transition in $R_{1+x}Ba_{2-x}Cu_3O_y$ (R = Nd, Sm, and Eu)," Phys. Rev. B **38**, 2450 (1988).

[17]E. A. Goodilin, N. N. Oleynikov, E. V. Antipov, R. V. Shpanchenko, G. Y. Popov, V. G. Balakirev, and Y. D. Tretyakov, "On the stability region and structure of the $Nd_{1+x}Ba_{2-x}Cu_3O_y$ solid solution," Physica C **272**, 65–78 (1996).

[18]M. Gombos, E. Varesi, P. Tedesco, A. Vecchione, and S. Pace, "A simple statistical phenomenological model for cation substitutions in $Nd_{1+x}Ba_{2-x}Cu_3O_{7-\delta+x/2}$," Philos. Mag. **88**, 1389–1399 (2008).

[19]M. Murakami, S. I. Yoo, T. Higuchi, N. Sakai, M. Watabiki, N. Koshizuka, and S. Tanaka, "A new type of pinning center in melt-grown Nd123 and Sm123," Physica C **235–240**, 2781 (1994).

[20]V. V. Petrykin, E. A. Goodilin, J. Hester, E. A. Trofimenko, M. Kakihana, N. N. Oleynikov, and Y. D. Tretyakov, "Structural disorder and superconductivity suppression in $NaBa_2Cu_3O_z$ ($z \sim 7$)," Physica C **340**, 16–32 (2000).

[21]M. Gombos, V. Gomis, A. E. Carrillo, A. Vecchione, P. Tedesco, S. Pace, and X. Obradors, "Reactivity between $Nd_{1+x}Ba_{2-x}Cu_3O_{7-\delta+x/2}$ and $Nd_{4-2z}Ba_{2+2z}Cu_{2-z}O_{10-2z}$ phases in superconducting NdBaCuO powders and melt textured bulk samples," Supercond. Sci. Technol. **16**, 865–871 (2003).

[22]W. Bieger, G. Krabbes, P. Schatzle, L. Zelenina, U. Wiesner, P. Verges, and J. Klosowski, "The Influence of initial composition and oxygen partial pressure on the properties of melt-textured NdBaCuO," Physica C **257**, 46 (1996).
[23]A. Vecchione, P. Tedesco, M. Gombos, M. Polichetti, and S. Pace, "Directional solidification in air of NdBaCuO bulk superconductor," Inst. Phys. Conf. Ser. **167**, 143–146 (2000).
[24]V. Gomis, M. Gombos, A. E. Carrillo, J. Plain, X. Obradors, S. Pace, and A. Vecchione, "Top seeding growth and microstucture of large grain Nd123/422 superconductors," Inst. Phys. Conf. Ser. **167**, 83–86 (2000).
[25]L. Bauernfeind, W. Widder, and H. F. Braun, "Superconductors consisting of CuO_2 and RuO_2 layers," J. Low Temp. Phys. **105**, 1605 (1996).
[26]L. Marchese, A. Vecchione, M. Gombos, C. Tedesco, A. Frache, H. O. Pastore, S. Pace, and C. Noce, "Structure and morphology of $NdSr_2RuCu_2O_y$ and $GdSr_2RuCu_2O_z$," Springer Verlag Lect. Notes Phys. **603**, 205–221 (2002).
[27]A. Vecchione, M. Gombos, C. Tedesco, A. Immirzi, L. Marchese, A. Frache, C. Noce, and S. Pace, "Synthesis, morphology and structural properties of $(Gd,Nd)Sr_2RuCu_2O_x$ samples," Int. J. Mod. Phys. B **17**, 899–904 (2003).
[28]C. Bernhard, J. L. Tallon, C. Niedermeier, T. Blasius, A. Golnik, E. Brücher, R. K. Kremer, D. R. Noakes, C. E. Stronach, and E. J. Ansaldo, "Coexistence of ferromagnetism and superconductivity in the hybrid ruthenate-cuprate compound $RuSr_2GdCu_2O_8$ studied by muon spin rotation and dc magnetization," Phys. Rev. B **59**, 14099 (1999).
[29]M. Cuoco, P. Gentile, M. Gombos, A. Vecchione, and C. Noce, "Coexistence of superconductivity and magnetism in ruthenocuprates," Adv. Sci. Tech. **67**, 182–191 (2010).
[30]A. Vecchione, M. Gombos, S. Pace, C. Tedesco, and D. Zola, "Crystal structures, magnetic, and superconducting properties of the $RuSr_2NdCu_2O_x$ and $RuSr_2GdCu_2O_y$ compounds," Physica C **372–376**, 1229–1231 (2002).
[31]J. Tallon, C. Bernhard, M. Bowden, P. Gilberd, T. Stoto, and D. Pringle, "Coexisting ferromagnetism and superconductivity in hybrid rutheno-cuprate superconductors," IEEE Trans. Appl. Supercond. **9**, 1696 (1999).
[32]A. C. McLaughlin and J. P. Attfield, "Tuning of the ferromagnetic and superconducting transitions by tin-doping in $RuSr_2GdCu_2O_8$," Phys. Rev. B **60**, 14605 (1999).
[33]J. W. Lynn, B. Keimer, C. Ulrich, C. Bernard, and J. L. Tallon, "Antiferromagnetic ordering of Ru and Gd in superconducting $RuSr_2GdCu_2O_8$," Phys. Rev. B **61**, R14964–R14967 (2000).
[34]K. Nakamura and A. J. Freeman, "Canted ferromagnetism in $RuSr_2GdCu_2O_8$," Phys. Rev. B **66**, 140405 (2002).
[35]A. Vecchione, D. Zola, G. Carapella, M. Gombos, S. Pace, G. Costabile, and C. Noce, "Low frequency transport measurements in $GdSr_2RuCu_2O_8$," Eur. Phys. J. B **31**, 151–157 (2003).
[36]A. Vecchione, D. Zola, C. Noce, G. Carapella, M. Gombos, G. Costabile, and S. Pace, "Analysis of AC transport measurements on $GdSr_2RuCu_2O_8$," Int. J. Mod. Phys. B **17**, 910–915 (2003).
[37]A. Vecchione, M. Gombos, C. Tedesco, D. Sisti, S. Uthayakumar, and S. Pace, "Effects of oxygenation processes on $(Nd,Gd)Sr_2RuCu_2O_x$ synthesis," Physica C **388–389**, 391–392 (2003).
[38]C. Tedesco, H. O. Pastore, A. Frache, M. Gombos, A. Immirzi, A. Vecchione, and L. Marchese, "A comparison of the processes involved in the direct synthesis of $GdSr_2RuCu_2O_x$ and $NdSr_2RuCu_2O_y$ perovskites," Physica C **408–410**, 193–194 (2004).
[39]R. Ciancio, M. Gombos, G. Grimaldi, A. Nigro, A. Vecchione, and S. Pace, "Impact of the starting powder composition on $GdSr_2RuCu_2O_8$ melt-textured processes," IEEE Trans. Appl. Supercond. **19**, 2945–2948 (2009).
[40]M. Gombos, A. Vecchione, R. Ciancio, D. Sisti, S. Uthayakumar, and S. Pace, "Melt-textured $GdSr_2RuCu_2O_x$ samples: Preliminary results," Physica C **408–410**, 189–190 (2004).
[41]R. Ciancio, M. Gombos, A. Vecchione, R. Fittipaldi, and S. Pace, "Morphological and structural study on $GdSr_2RuCu_2O_8$ melt-textured samples," IEEE Trans. Appl. Supercond. **15**, 3149–3152 (2005).
[42]S. I. Yoo, N. Sakai, H. Takaichi, T. Higuchi, and M. Murakami, "Melt processing for obtaining $NdBa_2Cu_3O_y$ superconductors with high T_c and large J_c," Appl. Phys. Lett. **65**, 633 (1994).
[43]D. Zola, I. A. Grimaldi, G. Carapella, S. Pace, and M. Gombos, "Intrinsic anisotropy of superconducting properties in $NdBa_2Cu_3O_7$ by analysis of single domain melt-textured samples" Superconductors Science and Technology (to be submitted).
[44]A. Vecchione, M. Gombos, P. Tedesco, and S. Pace, "Fabrication of neodymium-based superconducting bulk materials," Int. J. Mod. Phys. B **14**, 2670–2675 (2000).
[45]S. Uthayakumar, P. Santhosh, M. Gombos, S. Ramesh Babu, R. Jayavel, A. Vecchione, and S. Pace, "Physical properties and characterization of $RuSr_2GdCu_2O_8$ (Ru-1212) grown by top seeded melt textured technique," Mater. Sci. Eng. B **163**, 165–169 (2009).
[46]M. Gombos, A. Vecchione, P. Tedesco, D. Zola, U. Gambardella, and S. Pace, "Study of morphological and structural properties of multi-seeded NdBaCuO samples," IEEE Trans. Appl. Supercond. **11**, 3517–3520 (2001).
[47]M. Gombos, A. Vecchione, D. Zola, P. Tedesco, and S. Pace, "Study of structural properties and morphology of multi-seeded NdBaCuO bars," Physica C **372–376**, 1141–1144 (2002).
[48]M. Gombos, V. Gomis, A. E. Carrillo, A. Vecchione, S. Pace, and X. Obradors, "Identification of Nd163 phase in melt-textured $NdBa_2Cu_3O_{7+x/2-\delta}$ bulk samples," J. Mater. Res. **18**, 2050–2054 (2003).
[49]M. Gombos, V. Gomis, A. E. Carrillo, A. Vecchione, S. Pace, and X. Obradors, "Correlation between the formation of growth bands and Nd210 addition in $Nd_1Ba_2Cu_3O_{7-\delta}$ bulk samples," IEEE Trans. Appl. Supercond. **13**, 3169–3172 (2003).
[50]M. Gombos, V. Gomis, A. Vecchione, R. Ciancio, R. Fittipaldi, A. E. Carrillo, S. Pace, and X. Obradors, "Mechanical fragility and tri-dimensional crack structure in NdBaCuO top seeded and multi-seeded melt-textured samples," IEEE Trans. Appl. Supercond. **15**, 3137–3140 (2005).
[51]M. Gombos, V. Gomis, R. Ciancio, D. Zola, A. E. Carrillo, G. Carapella, A. Vecchione, M. Polichetti, S. Pace, and X. Obradors, "Reduced twinning efficiency and tri-dimensional crack structure in melt-textured $NdBa_2Cu_3O_{7-\delta}$ bulk samples fragmentation process," Supercond. Sci. Technol. **25**, 125017 (2012).
[52]M. Gombos, R. Ciancio, A. Vecchione, and S. Pace, "Thermal properties of $GdSr_2RuCu_2O_{8-\delta}$ based mixtures in the $GdSr_2RuO_6$–CuO pseudo-binary system," Physica C **460–462**, 522–523 (2007).
[53]M. Gombos, R. Ciancio, A. Vecchione, and S. Pace, "Thermal characterisation of $GdSr_2RuCu_2O_y$ based mixtures in the $GdSr_2RuO_6$–CuO pseudo-binary system," J. Mater. Res. **22**, 1579–1584 (2007).
[54]M. Gombos, A. Vecchione, D. Sisti, R. Ciancio, R. Masini, and S. Pace, "Gd-Nd solubility in the (Gd, Nd)-Sr-Ru-Cu-O system," IEEE Trans. Appl. Supercond. **17**, 2965–2968 (2007).
[55]V. S. Bagaev, S. I. Krasnosvobodtsev, A. G. Poiarkov, and E. G. Romanov, "Optical studies of YBCO c—Axis in plane oriented film in normal and superconductive states," Solid State Commun. **92**, 401–405 (1994).
[56]T. Dahm, D. Manske, and L. Tewordt, "Effect of a normal-state pseudogap on optical conductivity in underdoped cuprate superconductors," Phys. Rev. B **60**, 14888–14892 (1999).
[57]P. Dore, A. Paolone, S. Tatoni, C. P. Varsamis, V. Boffa, C. Romeo, S. Barbanera, and F. Murtas, "Extra-Drude contribution to the far-infrared conductivity oxygen-deficient YBCO films," Int. J. Infrared Millim. Waves **15**, 723–738 (1994).
[58]J. Orenstein, "Optical conductivity and spatial inhomogeneity in cuprate superconductors," in *Handbook of High-Temperature Superconductivity: Theory and Experiment*, edited by J. R. Schrieffer and J. S. Brooks (Springer, New York, 2007), pp. 299–324.
[59]T.-R. Tsai, C.-C. Chi, and S.-F. Horng, "Terahertz responses of high-resistivity YBCO thin films," Physica C **391**, 281–288 (2003).
[60]S. Pessaud, F. Gervais, D. deSousa, R. Lobo, C. Champeaux, P. Marchet, A. Catherinot, J. L. Longuet, and F. Ravel, "Optical conductivity of high-T_c cuprate thin films deposited by multi-target laser ablation," J. Phys.: Condens. Matter **12**, 1517–1525 (2000).
[61]W. J. Padilla, M. Dumm, S. Komiya, Y. Ando, and D. N. Basov, "Infrared signatures of hole and spin stripes in $La_{2-x}Sr_xCuO_4$," Phys. Rev. B **72**, 205101 (2005).